COMMUNICATION

Schiff-base [4]helicene Zn(II) complexes as chiral emitters

Mariia Savchuk,[†,a] Steven Vertueux,[†,a] Thomas Cauchy,[a] Mathieu Loumaigne,[a] Francesco Zinna,[b] Lorenzo Di Bari,[b] Nicolas Zigon*[a] and Narcis Avarvari *[a]

Received 00th January 20xx,
Accepted 00th January 20xx

DOI: 10.1039/x0xx00000x

The controlled preparation of chiral emissive transition metal complexes is fundamental in the field of circularly polarized luminescence (CPL) active molecular materials. For this purpose, Zn(II) complexes 1-3 based on the first tetradentate salen ligand surrounded by [4]helicene moieties and chiral 1,2-cyclohexane-diamines have been synthesized. The achiral complex 4 based on *ortho*-phenylene-diamine has been prepared as well. The optical and chiroptical properties of these complexes have been investigated and compared to DFT calculations.

Schiff base complexes derived from the salen ligand have been thoroughly explored for their unique properties.[1] Usually obtained by the condensation of a diamine with two equivalents of a salicylaldehyde derivative, they yield a versatile tetradentate ligand, that can be easily adapted in terms of steric hindrance and electronic properties. They attracted a particular deal of interest for their catalytic activity, in particular for epoxidation reaction with the well-known Jacobsen's catalyst based on a Mn(III)-salen complex, which was also successfully adapted for chiral catalysis.[2]

In addition to their use in catalysis, salen based complexes have drawn attention both for their magnetic properties,[3] especially when containing lanthanide ions,[4] or manganese (III)),[5] and their emissive properties.[6–9] Noteworthy, Zn(II) and Ni(II)-salen have been incorporated in LED devices.[10–13]

Our group has a long-lasting interest for chiral materials,[14] and, therefore, developed several compounds using the helicenic scaffold, which is an *ortho*-fused polyaromatic moiety.[15] Helicenes and heterohelicenes are renowned for their large magnitude of chiroptical properties, such as optical rotation (OR), electronic circular dichroism (ECD), vibrational circular dichroism (VCD) and circularly polarized luminescence (CPL).[16,17] Moreover, their combination with metal complexes has been explored to yield phosphorescent compounds.[18–20] Accordingly, we have designed electro- [21] and photo-active [22–24] helicene and heterohelicene compounds and investigated their properties.

Herein, we describe the first enantiopure Zn(II)-salen-helicene complexes together with their photophysical and chiroptical properties, supported by TD-DFT calculations. Using Zn(salen) complexes for their luminescence properties is also strongly attractive due to the Zn(II) earth abundancy and low price compared to heavier metals.

The original key building block **9** (Scheme 1) which we considered was a [4]helicene bearing an alcohol in the *ortho* position of an aldehyde group, thus reminiscent of salicylic-aldehyde, which is the proper configuration to assemble the tetradentate Schiff base. This design requires a precise stepwise construction of our precursor. For its synthesis, we have adapted procedures of phenol protection, Wittig type condensation, oxidative photocyclisation and aldehyde group

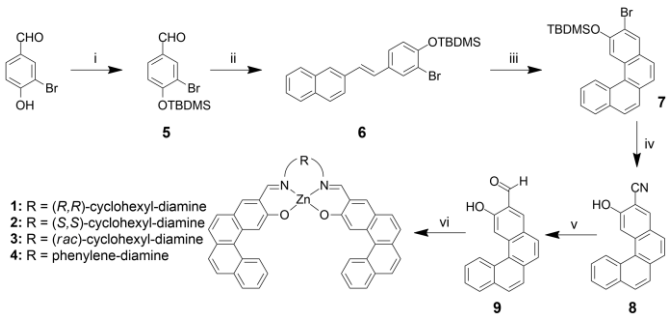

Scheme 1. Synthesis of the complexes **1**, **2**, **3** and **4**. i) TBDMSCl, imidazole, DMAP, DCM, RT, 70% ; ii) $C_{10}H_7CH_2PPh_3Br$, nBuLi, THF, -78°C to RT, 79% as a mixture of Z and E isomers; iii) hν, I_2, propylene oxide, toluene, 53% ; iv) μ-wave, CuCN, NMP, 95%; v) DIBAL-H, toluene, 53% ; vi) $Zn(OAc)_2$, diamine, MeOH, 73-95%.

[a] *Univ Angers, CNRS, MOLTECH-Anjou, SFR MATRIX, F-49000 Angers, France. E-mail: narcis.avarvari@univ-angers.fr*
[b] *Dipartimento di Chimica e Chimica Industriale, Università di Pisa, via G. Moruzzi 13, 56124, Pisa, Italy.*
† These authors contributed equally to this work.
Electronic Supplementary Information (ESI) available. CCDC 2080966–2080969. For ESI and crystallographic data in CIF or other electronic format see DOI: 10.1039/x0xx00000x

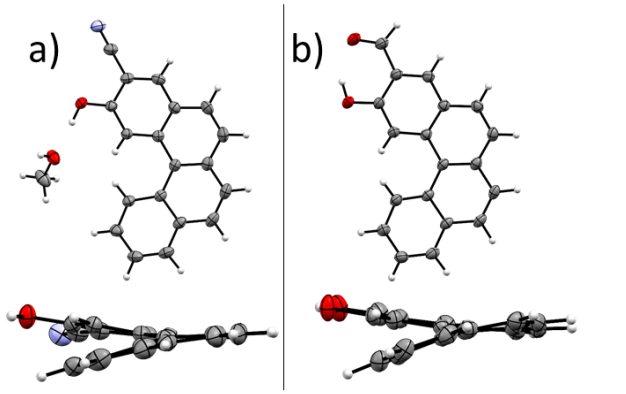

Figure 1. X-ray structures of a) compound **8** and b) compound **9**. (top : view perpendicular to the helix and bottom : side view of the helix). (Carbon: black ; Nitrogen : blue ; Oxygen : red ; Zinc : grey ; Hydrogen : white).

formation in a multi-step procedure (Scheme 1). The synthesis consists of five steps, with good global yields.

First, 3-bromo-4-hydroxybenzaldehyde was protected with a *tert*-butyldimethylsilyl group (TBDMS) to prevent side reactions during the following step, affording **5** with 70% yield. The protected aldehyde **5** was further reacted with 2-naphthyl-methyltriphenylphosphonium bromide following a classical Wittig protocol to obtain the stilbene **6** as a mixture of Z/E isomers with 79% yield. Photocyclisation in diluted conditions using a stoichiometric amount of I_2 and propylene oxide as proton scavenger afforded **7**.

Although direct formylation reaction by lithium bromide exchange and addition of DMF was attempted - varying the solvents, temperature and reaction time - it yielded only the debrominated helicene. Compound **7** was therefore further reacted following a Rosenmund-von Braun reaction under microwave activation in N-methyl-pyrrolidone[25] to obtain the cyanated [4]helicene **8**. Satisfyingly, the TBDMS protecting group was simultaneously removed, presumptively because of the Lewis acid character of CuCN. The corresponding aldehyde **9** was obtained by reduction with DIBAl-H in THF.

Crystals of compound **8** suitable for X-ray analysis were obtained by slow evaporation of a $CHCl_3/CH_3OH$ solution (Fig. 1). The compound crystallized in the monoclinic space group $P2_1/n$, with one helicene and a MeOH molecule in the asymmetric unit connected by a H-bond between the two alcohol functions ($d_{O\text{-}O}$ = 2.658(1) Å). Due to the symmetry operations, both *P* and *M* enantiomers are observed in the structure. The dihedral angle in the helicene moiety is equal to 22.5°. Compound **9**, for which single crystals have been obtained by slow diffusion of CH_3OH in a CH_2Cl_2 solution of the

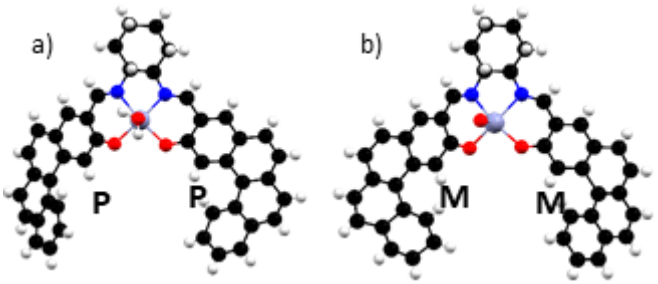

Figure 2. X-ray structure of complex **1** showing the two independent molecules. (Carbon: black ; Nitrogen : blue ; Oxygen : red ; Zinc : grey ; Hydrogen : white).

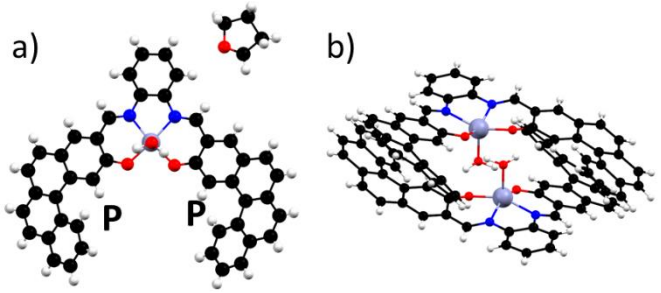

Figure 3. X-ray structure of complex **4**. a) Asymmetric unit and b) H-bonded dimer observed in the solid state.

compound, crystallized as well in the monoclinic space group $P2_1/n$. Again, both *P* and *M* enantiomers are present in the structure. The dihedral angle between terminal benzene rings is equal to 27.1°. π–π stacking occurs between helicenes, creating enantiopure columnar stacks separated by 3.35 Å between the functionalized benzene rings. An intramolecular H-bond is observed between the alcohol hydrogen and the oxygen of the aldehyde moiety, with an O-H-O angle of 148(3)° and a O-O distance of 2.674(2) Å.

Finally, the target salen complexes **1**-**4** were synthesized by a one-pot reaction with diamine, $Zn(OAc)_2$ and **9** in MeOH in good yields (Scheme 1). Model salen complexes **10**-**12** (see the ESI), with benzene instead of [4]helicene, were synthesized for comparison reasons according to reported literature procedures by condensation of salicyladehyde, diamine and $Zn(OAc)_2$ in MeOH.[26] As assessed by single crystal X-Ray diffraction, complexes **1** and **4**, bearing two [4]helicene moieties, display the typical tetradentate O,N,N,O coordination around Zn(II) characteristic of salen ligands. Single crystals of complexes **1** and **4** were obtained by vapour diffusion of MeOH in a solution of the compound in THF at room temperature. The dataset for **1** stands below the iUCr standards despite numerous crystallization trials and an extended X-Ray irradiation time, and therefore the precise bond lengths and bond angles values will not be discussed here. Complex **1** crystallized in the non-centrosymmetric monoclinic space group *P*2. In the solid state, the Zn atom is pentacoordinated by the tetradentate O,N,N,O Schiff base and one apical water molecule in a square pyramidal conformation. Two molecules are observed in the asymmetric unit, both having two asymmetric *R,R* carbons in the cyclohexyl-diamine moiety. The first molecule displays *P,P* configuration for the helicene moiety, while the second molecule displays a *M,M* configuration (Fig. 2). They tend to associate into dyads through H-bonding interactions of the apical water molecule with their symmetrical counterparts (see the ESI). Complex **4** crystallizes in the centrosymmetric monoclinic space group $P2_1/c$ (Fig. 3). As for **1** the Zn ion is surrounded by the square defined by the tetradentate Schiff base, and bears a water molecule in its apical position. The Zn atom lies slightly above the plane formed by the four O,N,N,O atoms, thus adopting a distorted square pyramidal conformation. One molecule contains two helicene moieties with a similar configuration: either *P,P* or *M,M.* A THF molecule completes the structure. *P,P* and *M,M* molecules are connected by four hydrogen bonds between the hydrogens of the apical water molecule and the

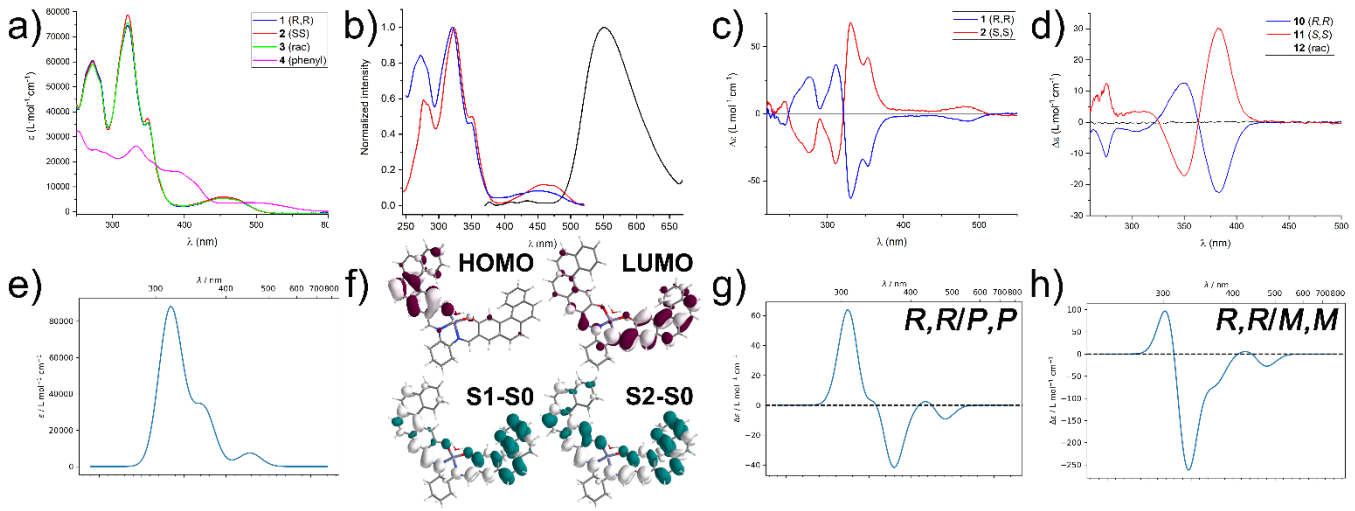

Figure 4. UV-visible spectra of the a) complexes **1-4** (THF, 10^{-5} M), b) normalized emission and excitation spectra (λ_{em} = 350 nm ; λ_{exc} = 530 nm) of complex **3** (THF, 10^{-5} M range, blue: absorption ; red: excitation ; black : emission), c) ECD spectra of complexes **1** and **2** (THF, 1-1.5·10^{-5} M range), d) ECD spectra of model complexes **10-12** (DMSO, 2-3.10^{-5} M range), e) calculated UV-visible spectra for complex **1**, f) frontier molecular orbitals of **1** and representation of the Electron Density Difference (S1-S0 - left) and (S2-S0 - right), calculated circular dichroism spectra for complex **1** with helicene moieties in the g) *P,P* and h) *M,M* conformations.

oxygens of the salen moiety, with O···O distances in the 2.6-2.7 Å range, and O-H-O angles of 129° and 152°.

UV-visible spectra of the complexes were measured in THF solutions at 10^{-5} M and were compared with the theoretical spectra resulted from TD-DFT calculations using Gaussian with the PBE1PBE functional and a def2SVP basis set. The X-ray structure was used as a basis for atomic positions, which were further optimized. Experimentally, for complexes **1-3** wide absorption band are observed with maxima at 273 nm (ε = 60000 L·mol^{-1}·cm^{-1}), 322 nm (ε = 78000 L·mol^{-1}·cm^{-1}) and 350 nm (ε = 38000 L·mol^{-1}·cm^{-1}) which can be attributed to π–π* transitions in the aromatic moieties. Both the position and the overall ε values are in good agreement with the calculations. A further broad absorption band is observed for complexes **1-3** at 454 nm (ε = 6500 L·mol^{-1}·cm^{-1}), which can be attributed to an ILCT character. The UV spectrum of complex **4** is much less structured, owing to the presence of the extra phenyl rings of the diamine and in this case the most red-shifted absorption is found at 483 nm (ε = 3700 L·mol^{-1}·cm^{-1}). HOMO and LUMO orbitals, calculated for **1** in the *R,R/M,M* configuration, involved in this low energy transition, are represented in Fig. 4f. It is worth noting that for both *R,R/M,M* and *R,R/P,P* configurations HOMO-1/HOMO and LUMO/ LUMO+1 are degenerated and participate in both the S1 and S2 transitions (ESI). The electron density difference maps (Fig. 4f) between S1-S0 and S2-S0 are helpful here to understand the transitions, which are mostly consisting of a transfer of electronic density involving the salen and the helicene units. The difference in stability between the two diastereomers is not big enough to hypothesize that a helicene configuration would be favored in solution.

For all complexes **1-4** the excitation spectrum is very similar to the absorption one, whereas the emission for **1-3** has a maximum at 550 nm and for **4** at 620 nm (Fig. 4b and ESI). Complexes **1-3** have moderate quantum yields in the 10-16% range, while the phenyl derivative **4** displays only a 2.5% quantum yield (using quinine sulfate in 0.1M H_2SO_4 as a reference). Two lifetimes are displayed for each complex: a first one in the 1-1.6 ns range, and a second one of 3.1 ns (complex **4**) and around 5.4-6.0 ns for complexes **1-3** (Table S1 in the ESI), all properly fitted to the experimental TCSPC values using a bi-exponential function. The obtained values are in accordance with previously reported data, and could be explained by the competition between a π*-π and a CT transition.[27,28] The excitation spectra present a perfect match with the absorption spectra for the four complexes (Fig. 4b and ESI).

Thanks to the chiral diamine moiety, the complexes **1** and **2** are active in circular dichroism (Fig. 4c). For the sake of comparison, in order to disclose between a possible participation of the [4]helicene moieties and that of the chiral salen complex to the CD spectra, chiroptical properties of complexes **10** and **11** have been measured as well. They display a relatively strong response in CD (Fig. 4d). Interestingly, the charge transfer band involving the aromatics in the helicene moiety around 450-500 nm is CD active, with Δε of -5 L·mol^{-1}·cm^{-1} for **1** and 5 L·mol^{-1}·cm^{-1} for **2** at 480 nm, very likely resulting from an exciton coupling between the two helicene chromophores. Based on the structure of (*R,R*)-diaminocyclohexane, one can predict a negative couplet, with a crossover point at about 454 nm, a negative band at longer wavelengths and a positive one at shorter ones. This is indeed found in the experiment, where the positive component of the couplet is cancelled by the negative tail of the 330-360 nm system of CD bands. In the calculations (Fig. 4g and 4h and ESI) this couplet is much more evident. The ECD bands around 450-500 nm are absent in the model

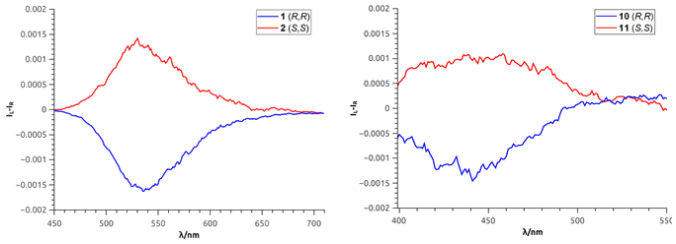

Figure 5. CPL spectra of (left) compounds **1-2** (~1·10^{-1} M in THF, λ_{exc} = 365 nm) and (right) model compounds **10-11** (~1·10^{-1} M in DMSO, λ_{exc} = 365 nm).

complexes **10** and **11**, which supports the active part taken by the extended aromatic moieties of **1** and **2** in the CD spectra. Furthermore, stronger signals with maxima at 353 and 330 nm are observed for **1** and **2**, with $\Delta\varepsilon$ absolute values of 39 and 63 $L{\cdot}mol^{-1}{\cdot}cm^{-1}$ respectively.

CPL associated to Zn-salen helicene compounds **1-2** was easily recorded thanks to a strong total luminescence and the absence of any significant photoselection. Complexes **1** and **2** display clear mirror image CPL signals with a maximum around 535 nm, retracing the fluorescence spectrum (Fig. 5). Dissymmetry factors g_{lum} around $+1.3{\cdot}10^{-3}$ and $-1.6{\cdot}10^{-3}$ were obtained at 535 nm for the *S,S* and *R,R* enantiomers, respectively. The sign is consistent with that observed for low energy ECD transitions (below 320 nm). The magnitude of the g_{lum} factors is in the usual range for transition metal complexes containing helicene units. Similarly, Zn-salen models **10** and **11** compounds show mirror image CPL signals with a maximum around 440 nm, retracing the fluorescence spectrum. Dissymmetry factors around $+1.1{\cdot}10^{-3}$ and $-1.3{\cdot}10^{-3}$, thus only slightly lower than the helicenic complexes, were obtained at 440 nm for the *S,S* and *R,R* enantiomers, respectively. Again, the sign is consistent with the one of the most red-shifted ECD transitions.

The dissymmetry factors obtained in both cases are in line with previous reports on Zn-salen CPL.[13] The CPL brightness defined by **Equation 1** was calculated [29]:

Equation 1 : $B_{CPL} = \frac{\varepsilon \times \Phi \times |g_{lum}|}{2}$

Complexes **1**, **2, 10** and **11** have B_{CPL} of 1.2, 0.8, 1.8 and 1.3 $L{\cdot}mol^{-1}{\cdot}cm^{-1}$ respectively. This places **1** and **2** below the average organic helicene values of 18.7 $L{\cdot}mol^{-1}{\cdot}cm^{-1}$ for CPL brightness, but on the high side of the range of the reported average values for *d*-Metal based compounds, which are 0.14, 0.79 and 1.0 $L{\cdot}mol^{-1}{\cdot}cm^{-1}$ for Re(I), Ir(III) and Pt(II) complexes respectively.[29]

In summary, we reported here the first synthesis and characterization of Schiff base Zn(II) complexes incorporating a helicenic scaffold. They exhibit excellent optical properties as fluorescent materials and display chiroptical activity.

The stereochemistry imposed by the chiral diamine is partially transferred to the helicene scaffold in solution and observed in electronic circular dichroism. Bi-exponential decrease of the luminescence lifetime is observed with two lifetimes in the range of 1-2 and 5-6 ns, respectively along with a QY in the 15% range. CPL is in the expected range for the emission wavelength and intensity for the complexes as attested by the B_{CPL} values. The sign of the CPL signal is determined by the chirality of the diamine employed in the synthesis. Theoretical calculations support the observed optical properties. These Zn(salen) complexes could be explored for their chiral electroluminescence properties in the visible.[26] Extending the size of the helicene moiety to block its configuration is the most important development, which is underway in our groups.

The authors declare no conflict of interest.

Notes and references

1 C. J. Whiteoak, G. Salassa and A. W. Kleij, *Chem. Soc. Rev.*, 2012, **41**, 622–631.
2 T. Katsuki, *Adv. Synth. Catal.*, 2002, **344**, 131–147.
3 M. Andruh, *Chem. Commun.*, 2011, **47**, 3025–3042.
4 I. Ramade, O. Kahn, Y. Jeannin and F. Robert, *Inorg. Chem.*, 1997, **36**, 930–936.
5 B. J. Kennedy and K. S. Murray, *Inorg. Chem.*, 1985, **24**, 1552–1557.
6 C.-M. Che, C.-C. Kwok, S.-W. Lai, A. F. Rausch, W. J. Finkenzeller, N. Zhu and H. Yersin, *Chem. – Eur. J.*, 2010, **16**, 233–247.
7 Y. Hai, J.-J. Chen, P. Zhao, H. Lv, Y. Yu, P. Xu and J.-L. Zhang, *Chem. Commun.*, 2011, **47**, 2435–2437.
8 G. S. M. Tong, P. K. Chow, W.-P. To, W.-M. Kwok and C.-M. Che, *Chem. – Eur. J.*, 2014, **20**, 6433–6443.
9 X. Yang, R. A. Jones and S. Huang, *Coord. Chem. Rev.*, 2014, **273–274**, 63–75.
10 G. Yu, Y. Liu, Y. Song, X. Wu and D. Zhu, *Synth. Met.*, 2001, **117**, 211–214.
11 O. Lavastre, I. Illitchev, G. Jegou and P. H. Dixneuf, *J. Am. Chem. Soc.*, 2002, **124**, 5278–5279.
12 A. C. W. Leung, J. H. Chong, B. O. Patrick and M. J. MacLachlan, *Macromolecules*, 2003, **36**, 5051–5054.
13 Y. Chen, X. Li, N. Li, Y. Quan, Y. Cheng and Y. Tang, *Mater. Chem. Front.*, 2019, **3**, 867–873.
14 F. Pop, N. Zigon and N. Avarvari, *Chem. Rev.*, 2019, **119**, 8435–8478.
15 Y. Shen and C.-F. Chen, *Chem. Rev.*, 2012, **112**, 1463–1535.
16 M. Gingras, *Chem. Soc. Rev.*, 2013, **42**, 1051–1095.
17 K. Dhbaibi, L. Favereau and J. Crassous, *Chem. Rev.*, 2019, **119**, 8846–8953.
18 J. R. Brandt, X. Wang, Y. Yang, A. J. Campbell and M. J. Fuchter, *J. Am. Chem. Soc.*, 2016, **138**, 9743–9746.
19 Z. Yan, X. Luo, W. Liu, Z. Wu, X. Liang, K. Liao, Y. Wang, Y. Zheng, L. Zhou, J. Zuo, Y. Pan and H. Zhang, *Chem. – Eur. J.*, 2019, **25**, 5672–5676.
20 E. S. Gauthier, L. Abella, N. Hellou, B. Darquié, E. Caytan, T. Roisnel, N. Vanthuyne, L. Favereau, M. Srebro-Hooper, J. A. G. Williams, J. Autschbach and J. Crassous, *Angew. Chem. Int. Ed.*, 2020, **59**, 8394–8400.
21 T. Biet, A. Fihey, T. Cauchy, N. Vanthuyne, C. Roussel, J. Crassous and N. Avarvari, *Chem. – Eur. J.*, 2013, **19**, 13160–13167.
22 T. Biet, T. Cauchy, Q. Sun, J. Ding, A. Hauser, P. Oulevey, T. Burgi, D. Jacquemin, N. Vanthuyne, J. Crassous and N. Avarvari, *Chem. Commun.*, 2017, **53**, 9210–9213.
23 T. Biet, K. Martin, J. Hankache, N. Hellou, A. Hauser, T. Bürgi, N. Vanthuyne, T. Aharon, M. Caricato, J. Crassous and N. Avarvari, *Chem. – Eur. J.*, 2017, **23**, 437–446.
24 A. Abhervé, K. Martin, A. Hauser and N. Avarvari, *Eur. J. Inorg. Chem.*, 2019, **2019**, 4807–4814.
25 J. Žádný, P. Velíšek, M. Jakubec, J. Sýkora, V. Církva and J. Storch, *Tetrahedron*, 2013, **69**, 6213–6218.
26 F. Dumur, L. Beouch, M.-A. Tehfe, E. Contal, M. Lepeltier, G. Wantz, B. Graff, F. Goubard, C. R. Mayer, J. Lalevée and D. Gigmes, *Thin Solid Films*, 2014, **564**, 351–360.
27 I. Majumder, P. Chakraborty, S. Dasgupta, C. Massera, D. Escudero and D. Das, *Inorg. Chem.*, 2017, **56**, 12893–12901.
28 D. Majumdar, S. Das, R. Thomas, Z. Ullah, S. S. Sreejith, D. Das, P. Shukla, K. Bankura and D. Mishra, *Inorg. Chim. Acta*, 2019, **492**, 221–234.
29 L. Arrico, L. Di Bari and F. Zinna, *Chem. – Eur. J.*, 2021, **27**, 2920–2934.

